

PAPER • OPEN ACCESS

An experimental investigation of the hydrodynamic damping of vibrating hydrofoils

To cite this article: C W Bergan *et al* 2019 *IOP Conf. Ser.: Earth Environ. Sci.* **240** 062008

View the [article online](#) for updates and enhancements.



IOP | ebooks™

Bringing you innovative digital publishing with leading voices to create your essential collection of books in STEM research.

Start exploring the collection - download the first chapter of every title for free.

An experimental investigation of the hydrodynamic damping of vibrating hydrofoils

C W Bergan¹, E O Tengs^{1,2}, B W Solemslie¹, and O G Dahlhaug¹

¹ NTNU Vannkraftlaboratoriet, 7491 Trondheim

² EDR & Medeso AS, NO-1337 Sandvika

E-mail: carl.w.bergan@ntnu.no

Abstract. As Francis turbines are chasing a higher efficiency, while trying to accommodate a wider load region, turbine blade fatigue is becoming a more pronounced problem. Details of the Fluid-Structure Interaction (FSI) between the turbine blades and the passing water is necessary to accurately predict the dynamic behavior of a runner in the design phase. The dynamic behavior of the turbine blades is characterized by three properties: The added mass of the surrounding water, the increased stiffness due to passing water, and the hydrodynamic damping provided by the surrounding water. Of the aforementioned properties, the hydrodynamic damping is not yet fully understood. When the turbine blades are excited close to resonance, the damping of the vibrating system determines the vibrational amplitude, and is therefore important in order to estimate the lifetime of a runner. The hydrodynamic damping of passing water has been investigated in a simplified setup, where the turbine blades are represented by a 2D hydrofoil. Two separate hydrofoil geometries have been tested. The hydrofoils were mounted in a “fixed-beam” configuration, meaning that both the deflection and the angle at the fastening point is zero. This setup was chosen, since it is the way that turbine blades are fastened in a Francis runner, and should therefore give applicable results when performing modal testing. The hydrofoils were mounted without any angle of attack, and exposed to water velocities up to 28 m/s. Modal tests in the entire velocity regime indicates that the damping factor increases linearly with water velocity, but at different rates below an above lock-in. The damping factor is rapidly increasing when the velocity goes beyond that of lock-in. This behavior is observed for both hydrofoils, even if the magnitude of the vortex shedding is of different magnitude for the two. A slight increase in natural frequency was also observed with increasing velocity, due to a combination of a stiffening effect of the water passing over the deflected blade, and a reduced added mass effect, in that the amount of water that vibrates with the hydrofoil is diminished when the water velocity is sufficiently high, i.e. it is blown away. The measurements have been compared with CFD simulations, indicating that the observed trend does indeed continue up to at least 45 m/s, indicating that the results are applicable to the velocity regimes occurring in a prototype Francis runner

1. Introduction

In the current energy market, Francis turbines are expected to deliver power at high efficiency while accommodating a large range of operation [1, 2]. This has caused several high head Francis runners to fail due to blade cracking, caused by Rotor-Stator Interaction (RSI) [3]. Fatigue damage due to vibration is a complex phenomena, with several factors: The static (mean) stress, the amplitude of the vibration, and the frequency of vibration. Within this, the amplitude of vibration, and hence the amplitude of the stress, can determine whether a turbine will withstand



the load, or if it will fail during operation. It is therefore important to understand the underlying mechanics that determine the vibrational amplitudes in the RSI-caused vibrations.

A classic damped vibrating system with a single degree of freedom can be characterized by three key parameters: stiffness, mass and damping. If one considered the oscillating turbine blade as a classic damped vibrating system, these characteristics will be slightly modified, as the presence of flowing water adds to stiffness, mass and damping. These parameters have been extensively investigated, and the impact of water on the stiffness and mass is well understood [4, 5, 6, 7]. The effect on damping has received less attention in the past, but recent studies have been conducted, indicating that the damping is indeed affected by the moving water. The damping is a critical quantity to understand, as the vibration amplitude is sensitive to damping at resonance. Some investigations of this have been performed in recent years, but they are limited in the velocity range investigated. In addition, the behavior of fluid damping in the velocity range where the blade's natural frequency coincides with the shedding frequency, known as lock-in, has not been a point of focus.

This paper presents experimental results on two separate hydrofoils, and a comparison is made between the results and simulation efforts.

2. Materials and Methods

The experimental setup and data analysis methods are described in the following section. The numerical setup is briefly explained, for an in-depth description, see [8].

2.1. Experimental Setup

The experiments were conducted at the Waterpower Laboratory at the Norwegian University of Science and Technology (NTNU). The test set-up consisted of a 150 mm by 150 mm square channel, containing the hydrofoil in a fixed-beam configuration, i.e. fastened in both ends. An image of the test rig is shown in Figure 1



Figure 1. Image of the test rig.

The hydrofoils tested are illustrated in Figure 2. They are of the same width and cord length, but F0 has an asymmetric trailing edge, and a more blunt leading edge than F1 .

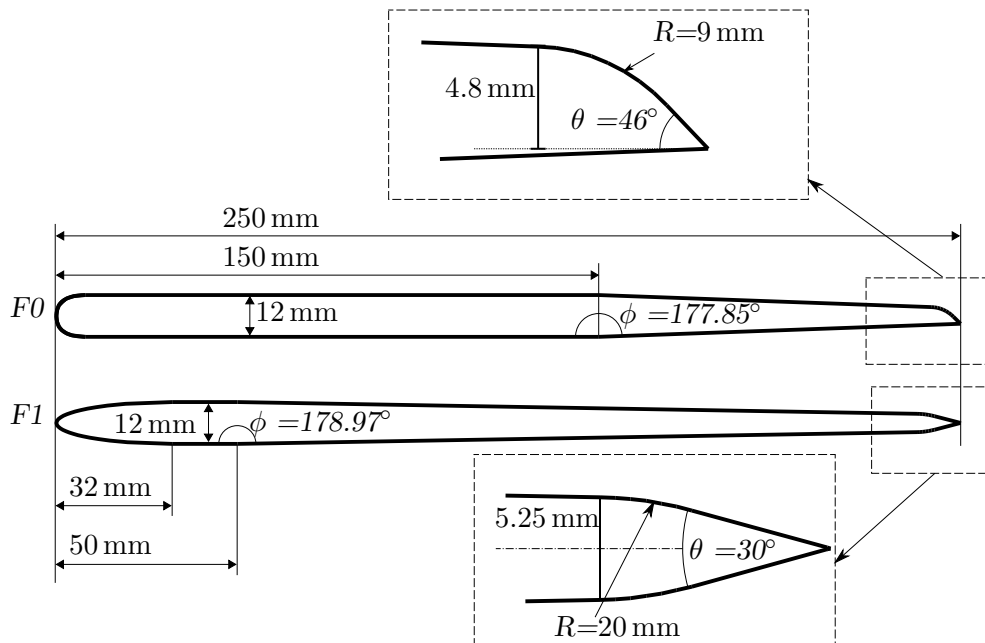


Figure 2. Hydrofoil geometries tested. Note that the tapering is much longer for F1 than for F0, allowing for a much smoother tapering angle, ϕ . In addition, F0 has an asymmetric trailing edge, while F1 has a symmetric trailing edge. The leading edge of F0 closely resembles a semicircle with diameter equal to the foil thickness, whereas the leading edge of F1 is elliptical with major and minor diameters of 62 mm and 12 mm respectively.

The excitation was performed using Piezoelectric Macrofiber Composites (MFCs), which have the ability to provide excitation at specific frequencies, enabling measurements when the damping is quite large. This procedure is based on the approach previously employed by Coutu et al, Yao et al, and Roth et al [4, 9, 10, 5, 6], and the MFCs are similarly excited 180° out of phase, in order to obtain the maximum excitation force. For a more in-depth explanation on the application of MFCs in conjunction with modal testing of hydrofoils, the reader is referred to the work of Seely et al [10]. The response was measured with a combination of Laser Doppler Vibrometry (LDV) and semiconductor strain gauges from Kulite. A schematic of the test setup is shown in Figure 3. The tests were performed in cavitation-free conditions.

2.1.1. Testing procedure In order to avoid transient effects, a stepped-sine excitation pattern was chosen, as recommended by Ewins [11]. The testing therefore consisted of

- (i) performing a continuous sweep, to identify the natural frequency
- (ii) generating discrete sine waves around the resonant region
- (iii) testing the response of each frequency

This process was repeated approx. 30 times for each velocity in order to estimate the uncertainty in both natural frequency and damping.

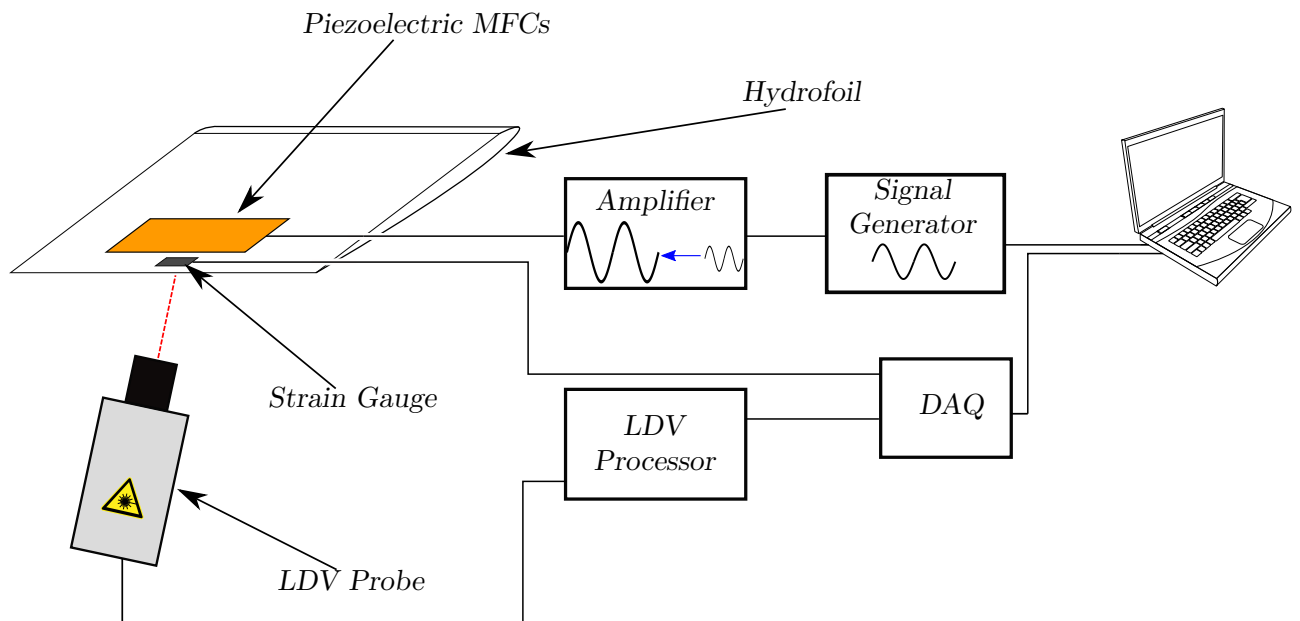


Figure 3. Schematic view of the measurement setup.

2.1.2. Analysis The amplitudes of both the excitation and response were calculated using the Welch method as implemented by MATLAB. The Welch method is an estimate of the power spectrum, which reduces the noise by reducing the frequency resolution through overlapping windows. For the amplitude estimates, the flattop window was chosen. Since the Welch method in MATLAB does not yield phase data, the phase difference between the excitation and response was estimated by calculating the cross-power spectral density. The magnitude ratio between the excitation and response, along with the phase difference was used to recreate the complex Frequency Response Function (FRF), which was used to calculate damping and natural frequency, using the nyquist diagram. By plotting the real part vs. the imaginary part of the FRF, a resonant region will appear as a circle. By curve fitting the data to a circle, geometric properties of the curve fit can be used to accurately estimate modal properties. This method was chosen, since it does not rely on data far away from the resonant region, and is therefore less sensitive to neighbouring modes of vibration. For a detailed explanation of the circle-fit method and the Nyquist diagram, the reader is referred to Ewins [11], and Bergan et al [12].

2.2. Numerical setup

The damping of F1 has been tested numerically using ANSYS CFX. To ensure fully developed flow conditions in the test section, the inlet of the test domain was extended in order to satisfy a common entrance length criterion of $L > 10 \cdot D_h$. Similarly, the test domain was extended downstream to avoid outlet conditions affecting the simulation results. The damping was found using a one-way coupling, but investigating the structural response in advance, and performing CFD on the blade with pre-determined vibration. For a more in-depth explanation of the numerical setup and results, the reader is referred to [8].

3. Results

In Figure 4, the damping factor ζ is shown with respect to the water velocity w . Figure 6 shows the evolution of the natural frequency ω_n of the hydrofoils with respect to w . The slope estimates for the evolution of the damping are summarized in Table 1

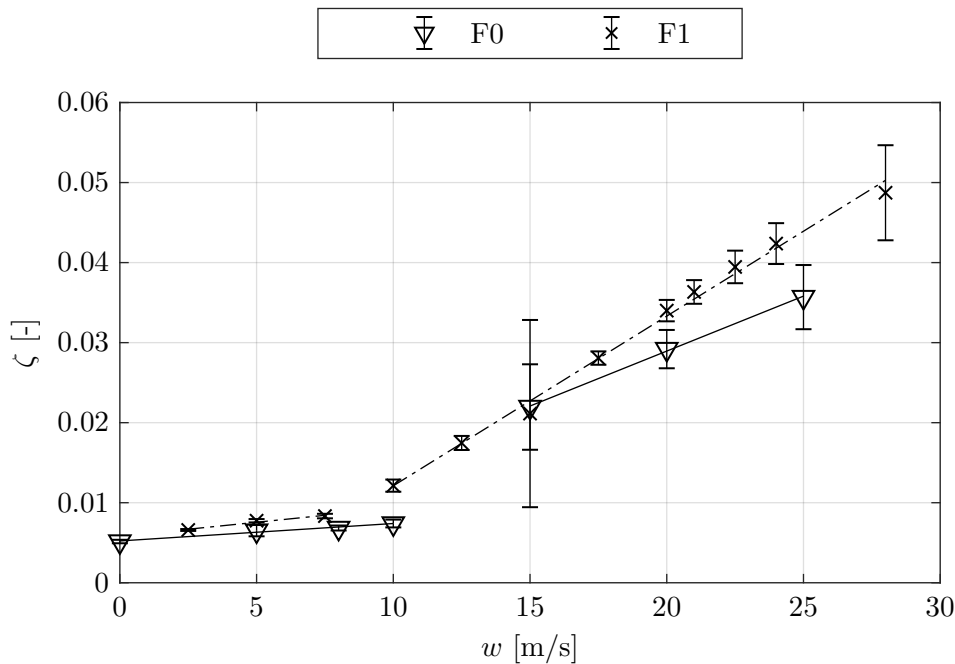


Figure 4. Damping vs velocity. Note that both hydrofoils exhibit a discontinuity in the slope around lock-in, at approx. 11 m/s for F0 , and at approx. 8 m/s for F1 .

Table 1. Slope of damping change vs. velocity

ζ/w	F0	F1
below lock-in	2.18×10^{-4}	3.48×10^{-4}
above lock-in	1.37×10^{-3}	2.12×10^{-3}

To give an idea of the numbers provided in table 1, the *Half-Amplitude* method is a useful tool [13]: A damping factor, ζ , of 0.01 (or 1%), means that oscillations will half in amplitude after 11 cycles, which for a hydrofoil with a natural frequency of 500 Hz is approx. 0.02 s.

The measurements are closely matched by the numeric simulations, shown in figure 5.

The experiments were limited to 28 m/s due to the onset of cavitation upstream the test section, even with a gauge pressure of 9 bar in the test section. Simulations were therefore conducted at 45 m/s, indicating that the trend obtained above lock-in continues.

As seen in Figure 4, the damping is nearly constant up to lock-in, but with a slightly positive slope. There is a distinct discontinuity, at approx. 11 m/s for F0 and at approx. 8 m/s for F1 . This is the lock-in region for each hydrofoil, the velocity at which the vortex shedding frequency coincides with the hydrofoil's natural frequency. This is detailed in table 2, where the maximum vibrational amplitudes are shown with and without MFC excitation. Vibration measured without MFC excitation is solely due to vortex shedding.

The natural frequency of the hydrofoils, as seen in Figure 6, seem to be relatively unaffected, but a closer investigation reveals a trend, see Figure 7.

Figure 7 shows that the natural frequency is not constant with velocity, it does in fact increase slightly with water velocity. F0 shows a sudden jump in natural frequency around lock-in, a

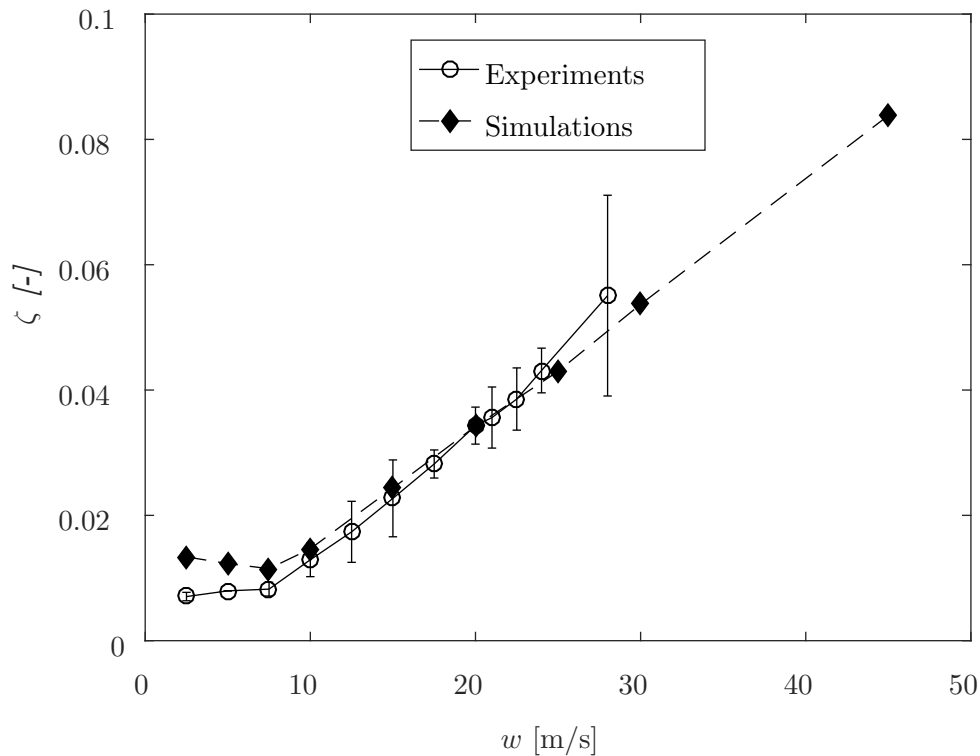


Figure 5. Experimental and numeric results for F1 . Note that both the experimental and numerical results indicate a change around the lock-in region (at 8 m/s), but they differ in the results below lock-in.

Table 2. Maximum Vibrational Amplitudes

Excitation Source	F0	F1
MFC	0.085 mm	0.125 mm
Vortex Shedding	0.013 42 mm	1.4×10^{-9} mm

behaviour that is not reflected in F1 . The order of increase seems to be quite similar as well, around a 0.1% increase for each m/s

The maximum vibrational amplitudes for F0 and F1 are shown in table 2. As the results indicate, the effect of vortex shedding is virtually non-existent for F1 , whereas the shedding-related vibrational amplitude for F0 is at approx. 16% of the maximum excited amplitude.

4. Discussion

The measurements were limited to 28 m/s due to cavitation, but the numerical analysis indicates that the trend is likely to continue at least up to 45 m/s, see figure 5. Given the similarities between the numerical and experimental results at velocities up to 28 m/s, there simulations performed at 45 m/s are most likely accurate.

At this stage, it is relevant to make comparison to other similar measurements, mainly those of Coutu et al [4], where a hydrofoil has been mounted in a fixed-beam configuration, and modal testing was done for velocities up to 25 m/s; and those of Yao et al [6], where the effect of the trailing edge shape was tested on a cantilever beam.

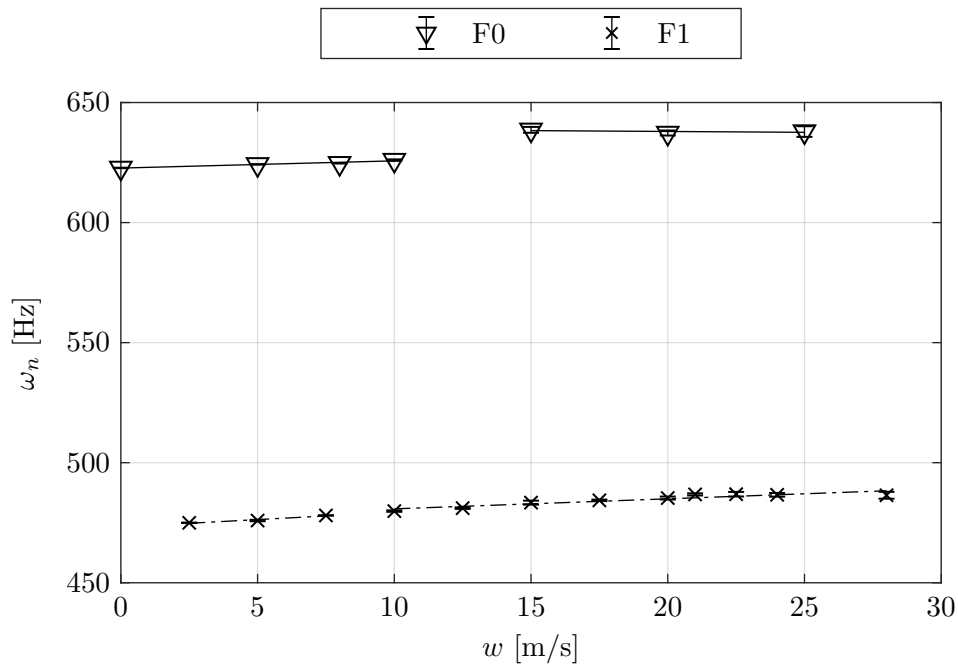


Figure 6. Natural Frequency. Note that there is a slight increase in natural frequency for both F0 and F1 .

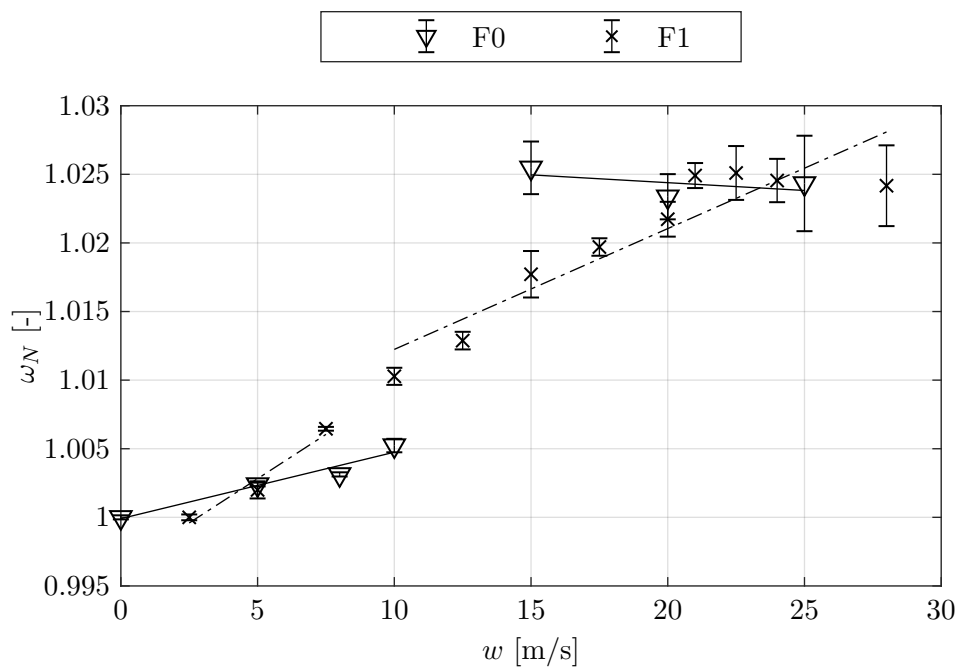


Figure 7. Normalized natural frequency. Note that both F1 and F0 appear to approach a constant value at 1.025.

Coutu et al found that the damping factor was consistently increasing with water velocity, without any discontinuities, but only above lock-in velocity. Comparing with Yao et al, a discontinuity in damping slope was observed at lock-in for the torsional bending mode, which for a cantilever beam is quite similar to the bending mode of a fixed-beam foil. Said discontinuity was observed at lock-in, which agrees very well with the trends observed in the present work.

In order to make a quantitative comparison to the results obtained by Yao et al, consider figure 8. Here, the damping is presented as a function of the *reduced velocity*, C^* , defined by Equation 1.

$$C^* = \frac{w}{L \cdot \omega_n} \quad (1)$$

As Figure 8 shows, the slope of the damping factor change is nearly identical for F0 and F1 when plotted against their reduced velocities. Compared with figure 9, it is clear that the observed damping behavior is similar in scale.

The slope of the damping change measured in the present work agree adequately with the measurements conducted by Yao et al, in which the slope of the damping was approx. 3.9×10^{-3} (when the velocity is expressed in absolute terms), as compared to approx. 2×10^{-3} obtained in this work. In the work of Coutu et al, the damping factor slope was found to be 1.07×10^{-2} to 1.23×10^{-2} , approx. 5 times higher than the results from this work. This result was fairly consistent for all the geometries tested by Coutu. Even if the geometry of the hydrofoils differ within each experiment, the dimensions for the test section remains.

Another key feature in the work of Yao is the apparent jump in natural frequency observed at lock-in, something that was also seen in the present measurements. Coutu et al found that the natural frequency remains constant, but CFD simulations performed by Nenneman et al [14] indicate that the natural frequency does indeed increase with velocity. The present results, and those of Yao, found that the natural frequency does change through the lock-in region, but there is no conclusive experimental evidence of further trends above lock-in. It could very well be the case that it is constant above lock-in.

Previous results have indicated that the phase shift in vortex shedding is the main contributor to the observed discontinuity in the evolution of the damping factor[12], but the present results contradict this. It is difficult to argue that the vortex shedding is the main contributor to the increase in damping when the same behavior is observed for both F0 and F1, even if the magnitude of the vortex shedding is quite different for the two test specimens.

The divergence in the present results, along with those of Coutu and Yao, raises the question of dimensionlessness: To what degree do we expect the damping factor to be dependent on the geometry and/or scale? Since the geometries in question differ, the proportion between the added mass and the blade stiffness is varying, which could cause different hydrodynamic behavior. It is also interesting to address the validity of the assumption of linearity in the vibrating system. Most theory regarding vibrating structures assume linearity, ie. spring force linearly proportional with displacement, damping force linearly proportional with velocity [13]. This may not be the case when the effects of FSI are prevailing[11]. There is lacking documentation on the effect of non-linearities in turbine blades, but the difference in scale between the prevailing experiments in this field suggest that the relative scale of the hydrofoil could be crucial to the expected rise in damping factor.

5. Conclusion

The present measurements show that the damping factor of a hydrofoil behaves differently above and below lock-in conditions, and the natural frequency is also affected by this. The two different test geometries indicate that a more slender blade might produce a lower natural frequency, having a reduced stiffness with the same oscillating mass, due to the larger relative

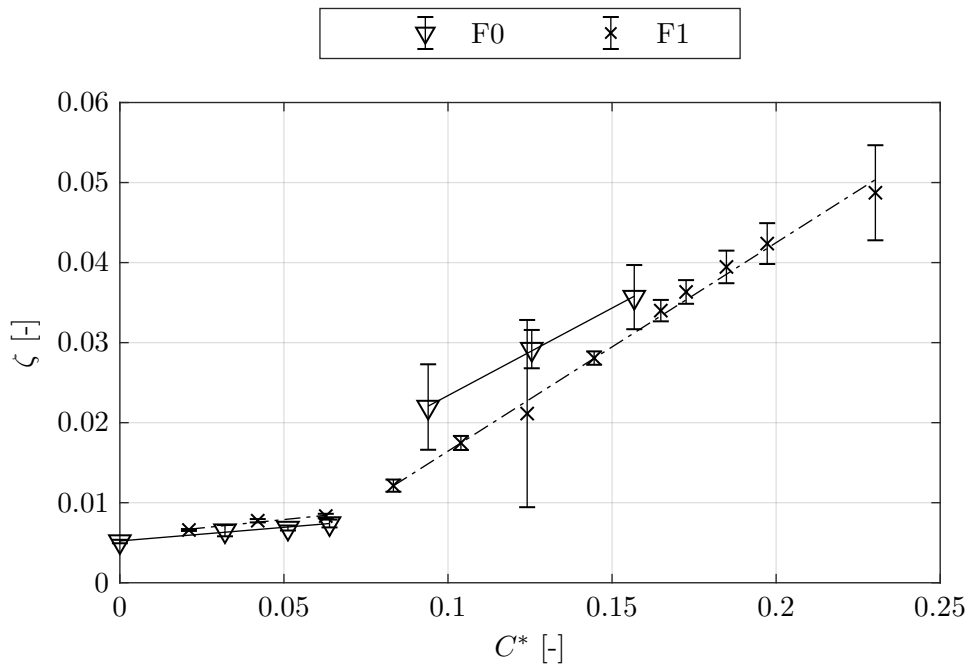


Figure 8. Damping vs reduced velocity.

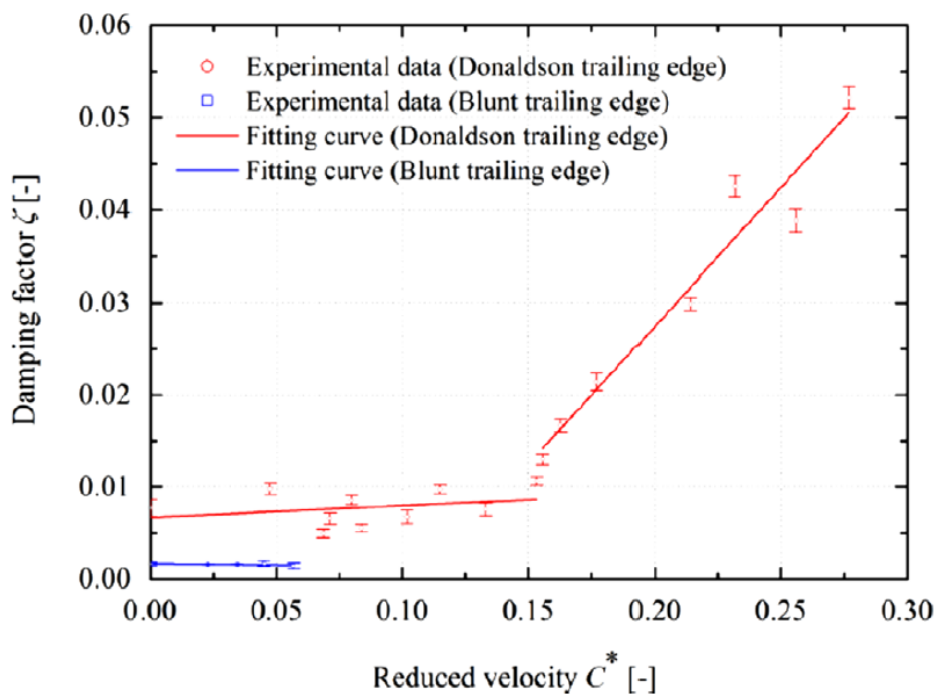


Figure 9. Measurements performed by Yao et al [6].

contribution from the water. Comparisons with similar experiments indicate that the increase in damping factor will be smaller for a stiffer hydrofoil, due to the reduced relative influence

of the fluid and the inherent non-linearities in a fluid-structure vibration. This could arguably be extended to encompass similar geometries of different scale, meaning that different types of turbines, with different relative blade thickness might have very different damping evolution with respect to the changing water velocities.

6. Further Work

Further investigations of damping behavior in submerged hydrofoils should include a thorough assessment of the linearity of the vibrating system. In addition, focus should be placed upon understanding the behavior of the natural frequency above lock-in, as the present measurements are inconclusive. Additionally, all the work performed on vibrating hydrofoils has focused on a single blade in vibration. Further measurements will encompass a multi-blade cascade, in order to capture influence from neighbouring blades.

7. Acknowledgements

The research was carried out as a part of HiFrancis, a high-head Francis turbine research program supported by the Norwegian Research Council, The Norwegian Hydropower industry, and the Norwegian Center for Hydropower.

References

- [1] Gagnon M and Thibault D 2015 *Proc. 6th IAHR International Meeting of the Workgroup on Cavitation and Dynamic Problems in Hydraulic Machinery and Systems*
- [2] Flores M, Urquiza G and Rodríguez J M 2012 *World J. Mech.* **2** 28–34
- [3] Trivedi C 2017 *Eng. Fail. Anal.* **77** 1 – 22
- [4] Coutu A, Seeley C, Monette C, Nennemann B and Marmont H 2012 *IOP Conf. Ser.: Earth Environ. Sci.* **15** 062060
- [5] Roth S, Calmon M, Farhat M, Münch C, Bjoern H and Avellan F 2009 *Proc. 3rd IAHR International Meeting of the Workgroup on Cavitation and Dynamic Problems in Hydraulic Machinery and Systems* **1** 253–260
- [6] Yao Z, Wang F, Dreyer M and Farhat M 2014 *J. Fluids Struct.* **51** 10. 189–198
- [7] Reese M C 2010 *Vibration and Damping of Hydrofoils in Uniform Flows* Master's thesis Pennsylvania State University
- [8] Tengs E O, Bergan C W, Jakobsen K R and Storli P T 2018 *Proc. 29th IAHR Symp. on Hydraulic Machinery and Systems (Kyoto) IAHR2018-033* (to be presented)
- [9] Monette C, Nennemann B, Seeley C, Coutu A and Marmont H 2014 *IOP Conf. Ser.: Earth Environ. Sci.* **22** 032044
- [10] Seeley C, Coutu A, Monette C, Nennemann B and Marmont H 2012 *Smart Mater. Struct.* **21** 035027
- [11] Ewins D J 2000 *Modal Testing: Theory, Practice, and Application* 2nd ed (*Mechanical engineering research studies* no 10) (Research Studies Press)
- [12] Bergan C W, Solemslie B W, Østby P and Dahlhaug O G 2018 *Int. J. Fluids Mach. Syst.* **11** 146–153
- [13] Craig R R, Kurdila A and Craig R R 2006 *Fundamentals of Structural Dynamics* 2nd ed (John Wiley)
- [14] Nennemann B, Monette C and Chamberland-Lauzon J 2016 *IOP Conf. Ser.: Earth Environ. Sci.* **49** 072006